

Metal–Metal Interactions in a Novel Hybrid Metallopolymer

Colin G. Cameron and Peter G. Pickup*

*Contribution from the Department of Chemistry, Memorial University of Newfoundland, St. John's, Newfoundland, Canada A1B 3X7**Received December 17, 1998. Revised Manuscript Received September 17, 1999*

Abstract: A conjugated polymer–redox polymer hybrid based on the complexation of poly[2-(2-pyridyl)-bibenzimidazole] with bis(2,2'-bipyridyl)Ru²⁺ has been prepared to take advantage of electronic communication between metal centers through the conjugated backbone. The existence of such communication is confirmed by the observation of an intervalence charge-transfer band in the near-IR spectrum of the Ru(III/II) mixed valence state. Electron transport studies by rotating disk voltammetry, dual (sandwich) electrode voltammetry, and impedance spectroscopy have yielded electron diffusion coefficients (D_e) of over 10⁻⁸ cm² s⁻¹ for the Ru(III/II) mixed valence state. D_e in nonconjugated Ru(2,2'-bipyridyl)₃^{3+/2+}-type polymers is typically less than this by at least a factor of 10, indicating that electron transport in the new polymer is enhanced by communication of metal centers through the backbone. The redox potential of the Ru sites, and D_e , can be manipulated by changing the electron density on the polymer backbone via pH control of the degree of protonation of the imidazole moieties.

Introduction

Chemically modified electrodes have been of interest because of their potential in electrocatalysis and other applications where deliberate control of the electrode–solution interface is desirable.^{1–3} The advantages over solution-based electrocatalysts may include (1) a higher effective concentration of catalyst than can be achieved in solution, (2) facilitated transfer of multiple redox equivalents to individual sites, (3) ease of extraction of the catalyst from the reaction medium, and (4) enhanced cooperative effects between catalyst components owing to small physical separation.

The use of polymers as supports for transition metal electrocatalysts is well-known.¹ Electrochemically polymerizable complexes provide a convenient route to polymer-supported catalysts although the resulting polymer need not necessarily be conjugated. Electropolymerized vinyl-substituted terpyridyl complexes of cobalt(II) for example have shown a number of interesting electrocatalytic properties such as the lowering of the reduction overpotential of O₂ by 300 mV, and that of CO₂ by nearly 1 V.⁴

Pyrrrole-substituted ligands have become popular in the preparation of polymerized metal complexes.⁵ With a π -conjugated backbone the rapid electron transfer typical of conducting polymers is reflected in such complexes. However, in these cases the metal complex is held at some distance from the backbone through a saturated link, leaving the metal electronically isolated from the π network. Modified electrodes of this type begin to consider the use of π conjugation as a means of enhancing electron transfer within the system; it is reasonable

to predict that highly efficient electrocatalysts must possess a facile means of shuttling electrons between the electrode surface and catalyst metal sites.

In this paper, we shall consider electron transport in a novel conjugated polymer–Ru complex hybrid. This class of materials, where metals are coordinated directly into a long-range π network, has only recently begun to attract significant attention, but the known examples have already exhibited a number of interesting properties.^{6,7} For example, Yamamoto and co-workers found that complexes of RuCl₃ with polypyridine and polybipyridine exhibit notable photocatalytic cleavage of water to H₂.⁸ Wolf and Wrighton⁹ have demonstrated that the electron density at a rhenium coordinated to a conjugated polymer, poly-[5,5'-(2-thienyl)-2,2'-bithiazole], can be modulated by the electron density of the polymer.

The anticipated advantage of an arrangement where the metal is coordinated into the π backbone lies in the premise that an interaction between metal-based $d\pi$ orbitals and ligand (polymer) $L\pi$ or $L\pi^*$ will occur. As a result, the π network can in essence act as an intramolecular electron conduit, allowing the rapid movement of electrons necessary for high electrocatalyst performance. The ability of conjugated linkages to provide an effective pathway for electron transfer between metal sites has been demonstrated in a number of polymeric systems. Zotti et al.¹⁰ have shown that electron-transfer rates between metal sites in polythiophenes with pendant ferrocene moieties are enhanced when a conjugated linkage is used. Zhu and Swager¹¹ demonstrated that the close match of the redox potentials of Cu^{2+/+} and an ethylenedioxythiophene–bipyridine copolymer leads to significant enhancement of the complexed polymer's conductivity.

* To whom correspondence should be addressed. E-mail: ppickup@morgan.ucs.mun.ca.

(1) Abruna, H. D. In *Electroresponsive Molecular and Polymeric Systems*; Skotheim, T. A., Ed.; Marcel Dekker: New York, 1991; pp 97–171.

(2) Durst, R. A.; Baumner, A. J.; Murray, R. W.; Buck, R. P.; Andrieux, C. P. *Pure Appl. Chem.* **1997**, *69*, 1317.

(3) Abruna, H. D. *Coord. Chem. Rev.* **1988**, *86*, 135.

(4) Arana, C.; Keshavarz, M.; Potts, K. T.; Abruna, H. D. *Inorg. Chim. Acta* **1994**, *225*, 285.

(5) Deronzier, A.; Moutet, J.-C. *Coord. Chem. Rev.* **1996**, *147*, 339.

(6) Kingsborough, R. P.; Swager, T. M. *Progr. Inorg. Chem.* **1999**, *48*, 123.

(7) Pickup, P. G. *J. Mater. Chem.* **1999**, *8*, 1641.

(8) Yamamoto, T.; Maruyama, T.; Zhou, Z.-H.; Ito, T.; Fukuda, T.; Yoneda, Y.; Begum, F.; Ikeda, T.; Sasaki, S.; Takezoe, H.; Fukuda, A.; Kubota, K. *J. Am. Chem. Soc.* **1994**, *116*, 4832.

(9) Wolf, M. O.; Wrighton, M. S. *Chem. Mater.* **1994**, *6*, 1526.

(10) Zotti, G.; Schiavon, G.; Zecchin, S.; Berlin, A.; Pagani, G.; Canavesi, A. *Synth. Met.* **1996**, *76*, 255.

(11) Zhu, S. S.; Swager, T. M. *J. Am. Chem. Soc.* **1997**, *119*, 12568.

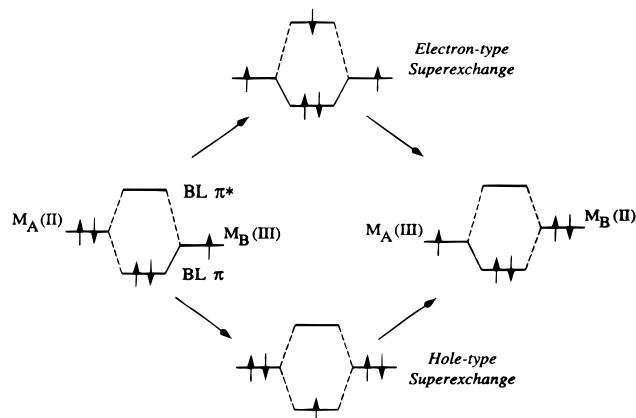
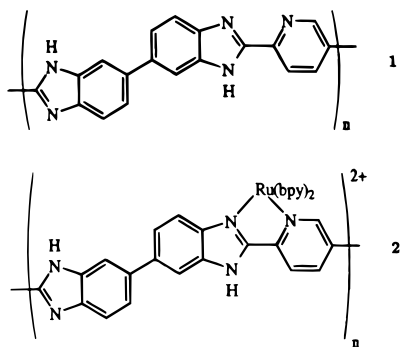


Figure 1. Proposed models for electron exchange through a π -conjugated bridging ligand (BL). (Adapted from ref 12.)

The essence of metal–ligand–metal interactions in a mixed valence conjugated bridging complex is shown schematically in Figure 1.¹² Two pathways are possible: (1) hole-type superexchange, where the ligand donates an electron from its HOMO to fill a $d\pi$ vacancy in the metal in the higher oxidation state, and the hole thus formed is filled by an electron from the other metal, and (2) electron-type superexchange, where an electron from the lower valence metal is promoted to the ligand π^* orbital, and subsequently falls into the other metal's $d\pi$ orbitals. The favored pathway will depend on the relative energy levels of the metal $d\pi$ orbitals and the bridging ligand's π/π^* orbitals, and the ease with which this exchange may occur depends on the absolute energy gap between the metal and ligand orbitals for the preferred pathway. It is anticipated that these bimetallic exchange mechanisms will be equally applicable to the extended conjugated bridging system in the present metallopolymer systems.

For the present study, we have chosen a Ru complex (**2**) of a pyridine–benzimidazole based polymer, poly[2-(2-pyridyl)-biphenyl] (**1**). A number of factors make this an



attractive choice: (1) polybenzimidazoles tend to be very robust,¹³ remaining stable under considerable thermal and chemical stress, (2) there is an excellent bidentate ligand site between the pyridine and imidazole nitrogen atoms, (3) the imidazole proton may be removed and replaced, affecting the electron density along the polymer backbone, and (4) similar binuclear complexes have been shown to possess notable coupling between the two metals.

Haga et al.^{12,14–20} have studied the electronic interaction of $\text{Ru}^{3+}/\text{Ru}^{2+}$ metal centers in a variety of benzimidazole-bridged complexes and the mixed valence stabilization resulting from

(12) Haga, M.; Ale, M. M.; Koseki, S.; Yoshimura, A.; Nozaki, K.; Ohno, T. *Inorg. Chim. Acta* **1994**, 226, 17.

(13) Vogel, H.; Marvel, C. S. *J. Polym. Sci.* **1961**, 50, 511.

the aforementioned superexchange processes. In the case of the dinuclear ruthenium complex **4** bridged by 2,2'-bis(2-pyridyl)-biphenyl, it was found that the electrochemistry and absorption spectra were dependent on solution pH, which dictates the protonation/deprotonation of the ligand imidazole N–H proton.¹⁴ Cyclic voltammetry suggested the presence of two closely spaced waves whose absolute position was determined by the pH. The authors estimated the peak separation to be ca. 45 mV for the protonated ligand, and nearly 80 mV for the deprotonated ligand. The separation of the two redox waves is related to the comproportionation constant K_{com} , which is a measure of stability of mixed valence complexes. It was concluded that the deprotonated ligand stabilizes the mixed valence state better, and this is probably due to the increase of the HOMO energy upon deprotonation.

Further evidence of enhanced intervalence transfer (IT) is shown in UV–vis–NIR spectra of the binuclear compounds.^{12,15} One-electron electrolysis of the binuclear complex results in the appearance of an IT band in the near-infrared. The IT absorption stems from the slight difference in the inner-shell and outer-shell environments of the metal centers, a consequence of their different oxidation states. The IT band is effectively a metal–metal charge transfer, and so the degree of electronic coupling may be evaluated from its position, half-height width, and intensity. While this optical property is descriptive of chromophore interactions in the charge transfer state, it should parallel the electrochemistry, which is also in essence controlled by the interaction of metal and ligand orbitals.

Experimental Section

Materials. 3,3'-Diaminobenzidine (Aldrich, 99%), 2,5-pyridinedicarboxylic acid (Aldrich, 98%), phosphorus pentoxide (Fisher), and 85% phosphoric acid (Anachemia) were used as received. $\text{Ru}(\text{bpy})_2\text{Cl}_2$ was prepared according to a literature method.²¹ Acetonitrile was distilled over calcium hydride. Tetraethylammonium perchlorate was prepared according to a literature method²² and triply recrystallized from water. All other chemicals were reagent grade or better and used as received.

Instrumentation. Unless stated otherwise, all potentials are reported against a SSCE reference electrode. Electrochemical experiments were performed using a Hokuto-Denko HA301 potentiostat with HB104 function generator, a Pine Instruments RDE4 bipotentiostat with Pine Instruments ASR analytical rotator, or a Solartron Schlumberger 1268 electrochemical interface and 1250 frequency response analyzer. Impedance spectra were acquired using Zplot software, while cyclic voltammograms and $i - E$ data were acquired through a Data Translations DT2801 analogue–digital converter card with software written in our lab.

UV–vis–NIR spectra were recorded with a Cary 5E spectrometer. NMR spectra were obtained on a GE–300NB 300 MHz spectrometer.

Synthesis. (a) Poly[2-(2-pyridyl)biphenyl] (1**).** Polyphosphoric acid was generated in situ by the reaction of 5.5 g of H_3PO_4

(14) Haga, M.; Ano, T.; Kano, K.; Yamabe, S. *Inorg. Chem.* **1991**, 30, 3843.

(15) Ohno, T.; Nozaki, K.; Haga, M. *Inorg. Chem.* **1992**, 31, 548.

(16) Xiaoming, X.; Haga, M.-aki. *J. Chem. Soc., Dalton. Trans.* **1993**, 2477.

(17) Haga, M.; Ano, T.; Ishizaki, T.; Kano, K. *J. Chem. Soc., Dalton. Trans.* **1994**, 263.

(18) Haga, M.; Ali, M. M.; Maegawa, H.; Nozaki, K.; Yoshimura, A.; Ohno, T. *Coord. Chem. Rev.* **1994**, 132, 99.

(19) Haga, M. A.; Ali, M.; Arakawa, R. *Angew. Chem., Int. Ed. Engl.* **1996**, 35, 76.

(20) Haga, M. A.; Ali, M. M.; Koseki, S.; Fujimoto, K.; Yoshimura, A.; Nozaki, K.; Ohno, T.; Nakajima, K.; Stufkens, D. *J. Inorg. Chem.* **1996**, 35, 3335.

(21) Lay, P. A.; Sargeson, A. M.; Taube, H. *Inorg. Synth.* **1986**, 24, 291.

(22) Sawyer, D. T.; Roberts, J. L. *Experimental Electrochemistry for Chemists*; Wiley: New York, 1974.

with 8.9 g of P₂O₅, which were stirred under nitrogen at 120 °C for 9 h and then cooled to room temperature. 3,3'-Diaminobenzidine (1.03 g, 4.8 mmol) and 2,5-pyridinedicarboxylic acid (0.82 g, 4.9 mmol) were added, and the mixture was stirred under nitrogen at 120 °C for 5.5 h. A further 4.9 g of P₂O₅ was added to the resultant dark red viscous liquid to compensate for water of condensation. The mixture was stirred at 125 °C for a further 24 h, and 160 °C for a further 43 h. The resulting red viscous liquid was cooled to room temperature and stirred in a large volume of water, and the solid polymer was collected by filtration. The polymer was re-suspended in a large volume of water for a minimum of 24 h and filtered, an additional three times, yielding an amorphous orange solid that was dried for 72 h in vacuo at 90 °C to give 1.44 g (4.67 mmol, 97% yield) of product.

Elemental analysis: Predicted for C₁₉H₁₁N₅·4.5H₂O: C 58.45; H 5.16; N 17.94; O 18.44. Found: C 58.33; H 4.11; N 17.48; O 18.24. Trace P was detected by electron microprobe analysis, and together with the low percent H found this suggests that some of the oxygen accounted for by water in the proposed formula is actually present as a phosphorus-containing species (e.g. H₃PO₄). The 300 MHz ¹H NMR (CF₃CO₂D + 5% D₂O) spectrum of the polymer (see Supporting Information) is consistent with the proposed structure.

(b) Bisbipyridylruthenium Complex of Poly[2-(2-pyridyl)bibenzimidazole] (2). *Caution! Perchlorates are potentially dangerous.* While no detonation tendencies have been observed in this compound, standard precautions should be taken. Ru(bpy)₂Cl₂ (0.0499 g, 103 μmol) and poly[2-(2-pyridyl)bibenzimidazole] (0.0319 g, 103 μmol/site) were refluxed together in 50 mL of glycerol for 24 h. The solution was cooled to room temperature, diluted with 50 mL H₂O, and filtered. To the dark orange filtrate was added several milliliters of saturated aqueous NaClO₄. A dark precipitate slowly formed. This was collected by filtration, rinsed with water, and air-dried at room temperature to give 0.0550 g of fine dark red-brown solid (70% yield).

Elemental analysis: Predicted for C₁₉H₁₁N₅(C₂₀H₁₆N₄Cl₂O₈Ru)_{0.82}·3H₂O: C 49.10; H 3.52; N 13.40; Ru 9.58. Found: C 49.49; H 3.30; N 12.99; Ru 9.20. Samples of **2** with similar composition and essentially the same spectroscopic, electrochemical, and electron transport properties were prepared on two separate occasions.

Gel permeation experiments were employed to establish that **2** was a true polymer with high molar mass. Using Sephadex G-75 (rated MM 1000–50000) as the stationary phase, solutions of polymer complex **2**, the dinuclear model complex **4**, and an osmium-based redox polymer, Os(bpy)₂(polyvinylpyridine)Cl₂ (courtesy of J.G. Vos), of known MM > 10⁵ were eluted individually with an aqueous methanol solution, slightly acidified with HCl. Both polymers were found to elute simultaneously with the solvent front, while the relatively low molar mass model compound was retained at the top of the column. We conclude that polymer **2** has a molar mass greater than 5 × 10⁴ g mol⁻¹. This is sufficiently high that the electrochemical and spectroscopic results reported here are characteristic of a material with effectively infinite chain length, since the electronic properties of conjugated systems are known to converge to approximately constant values for more than ca. 20 repeat units.²³

Film Preparation and Thickness. Films of **1** suitable for electrochemical study were cast from a solution in *N,N*-dimethylacetamide, while films of **2** were cast from solutions in water-saturated nitromethane.

The thickness, *d*, of films of **2** is a parameter necessary for the determination of the electron diffusion coefficient *D_e*. The surface coverage of ruthenium sites, Γ_{Ru}, is related to the charge, *Q*, passed in a slow sweep cyclic voltammogram of the Ru(III/II) wave, and the surface area *A* of the electrode:

$$\Gamma_{\text{Ru}} = Q/FA \quad (1)$$

The volume occupied by the Ru sites in the film is assumed to be comparable to that of Ru(bpy)₃(PF₆)₂. On the basis of this compound's crystal structure,²⁴ the concentration of Ru sites in the polymer, *C_{Ru}*, is estimated to be 1.6 × 10⁻³ mol cm⁻³. Hence, it is possible to estimate *d* from:

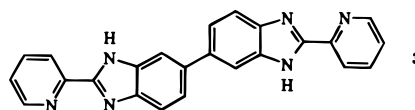
$$d = \Gamma_{\text{Ru}}/C_{\text{Ru}} \quad (2)$$

This approach has two significant shortcomings. First, the actual effective average volume of the Ru sites is likely somewhat larger than that of Ru(bpy)₃(PF₆)₂, and second, this estimate fails to consider any changes in thickness due to polymer swelling from solvent uptake. However, both of these flaws will tend to make the estimated *d* smaller than the true film thickness. This in turn means that calculated *D_e* values will underestimate the actual electron diffusion rate in the film (eq 6, vide infra). Scanning electron microscopic views of cross sections of polymer films deposited on ITO electrodes have shown that film thicknesses estimated in this manner are reasonable.

UV–Vis–NIR Spectroelectrochemistry. A relatively thick film of the polymer complex was cast onto a narrow slide of ITO-coated glass (Donnelly Corp.). The slide was then positioned inside a standard 1 cm quartz cuvette and held a short distance from the wall by an ca. 0.11 mm spacer. To minimize solvent absorption in the near-IR region, a small volume of 0.1 M Et₄NClO₄ in acetonitrile, acidified with HClO₄, was used so that the beam passed over the bulk of the solution, while a thin layer of solution could creep up the wall of the cuvette and cover the polymer film. A similar assembly, without polymer, was positioned in the reference beam. A Pt wire counter electrode and a Ag/AgCl reference electrode were used.

Results and Discussion

Poly[2-(2-pyridyl)bibenzimidazole] (1). Figure 2 shows UV–vis spectra of the poly[2-(2-pyridyl)bibenzimidazole] and a model compound, **3**. The polymer exhibits an absorption due



to the π–π* transition at λ_{max} = 401 nm in *N,N*-dimethylacetamide and at 427 nm in methanesulfonic acid. From the onset of these absorptions, the polymer band gap in these solvents is estimated at 2.8 and 2.4 eV, respectively. The red-shift accompanying protonation is consistent with spectra of the model compound and it has also been observed in other Schiff base polymers.²⁵ In going from the monomeric (**3**, λ_{max} = 343 nm) to the polymeric (**1**, λ_{max} = 401 nm) compound, the π–π* absorption shows a significant shift to longer wavelengths. This is consistent with the general trend of decreasing HOMO–LUMO gaps with increasing length of a π-conjugated system.

Cyclic voltammetry of a thin film of the uncomplexed polymer **1** in acetonitrile containing 0.1 M Et₄NClO₄ and following addition of acid or base is shown in Figure 3. In the neutral medium, there is a broad oxidation wave having an onset at around 1.0 V vs SSCE. The magnitude of the current decreases gradually with successive cycles (not shown). Over a wider range, an irreversible wave due to reduction of the polymer appears with an onset near –1.6 V. The electrochemical band gap (i.e. the energy difference between the onsets of oxidation and reduction) of ca. 2.6 eV agrees well with the optical band gap.

The cyclic voltammetric response of the polymer changes dramatically when acid (70% HClO₄(aq)) or base (Bu₄NOH as a 1 M solution in methanol) is added to the electrolyte solution (Figure 3). When a fresh film is cycled over the 0 to 1.4 V range first in neutral and then acidic electrolyte, the polymer immediately loses its current response. In basic media, the current becomes significantly larger after Bu₄NOH has been

(23) Jestin, I.; Frere, P.; Mercier, N.; Levillain, E.; Stievenard, D.; Roncali, J. *J. Am. Chem. Soc.* **1998**, *120*, 8150.

(24) Rillema, D. P.; Jones, D. S.; Levy, H. A. *Chem. Commun.* **1979**, 849.

(25) Yang, C. J.; Jenekhe, S. A. *Macromolecules* **1995**, *28*, 1180.

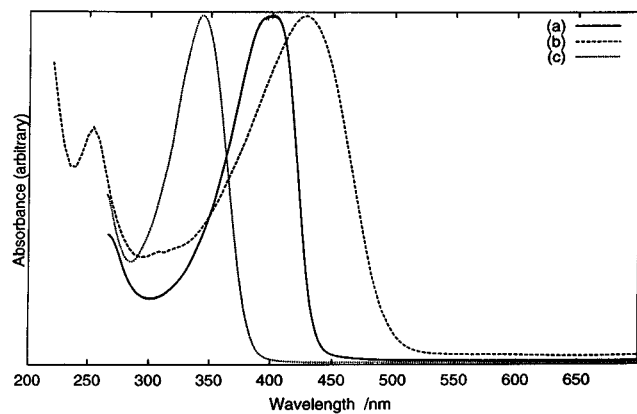


Figure 2. Electronic spectra of (a) **1** in *N,N*-dimethylacetamide, (b) **1** in methanesulfonic acid, and (c) **3** in *N,N*-dimethylacetamide.

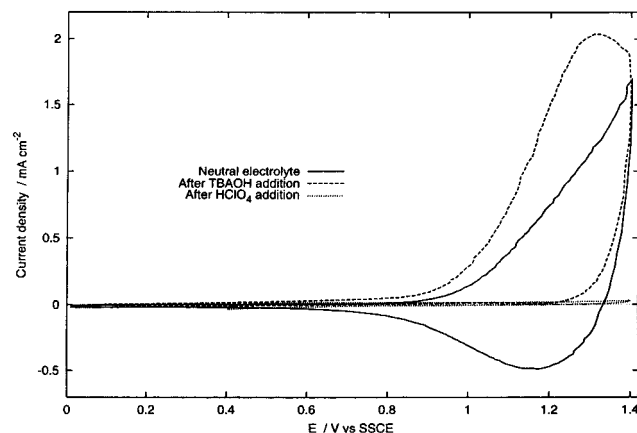


Figure 3. Cyclic voltammetry (100 mV s^{-1}) of the uncomplexed polymer **1** on a Pt disk electrode in acetonitrile containing $0.1 \text{ M Et}_4\text{NClO}_4$ (solid line), and following addition of HClO_4 (short dashes) or Bu_4NOH (long dashes).

added, but then degrades more rapidly than in the neutral solution. In addition, there is no cathodic (undoping) peak in base.

These results indicate that the electrochemical behavior of the uncomplexed polymer is influenced strongly by the protonation status of the imidazole and pyridine nitrogens. The loss of current on consecutive cycles indicates that the p-doped (oxidized) polymer is unstable, especially in the presence of base, presumably as a result of nucleophilic attack by water and/or OH^- .²⁶

Polymer Complex 2. Following coordination with $\text{Ru}(\text{bpy})_2^{2+}$, the UV-vis spectrum of the polymer (Figure 4) retains some features of the uncomplexed polymer. The intense $\pi-\pi^*$ transition is shifted only slightly, from 400 to 410 nm, although this might be partly attributable to the spectra having been acquired in different solvents. New absorptions at 246 and 287 nm are attributable to bipyridine transitions. A broad MLCT absorption appears as a shoulder on the large polymer $\pi-\pi^*$ peak, at ca. 510 nm. The spectrum of the polymer complex changes as a function of pH (Figure 4). In going from acidic to basic media, the intensity of the $\pi-\pi^*$ transitions in both the polymer and the bipyridine ligands decreases, while the MLCT transition grows in intensity. The change is fairly gradual, except between pH 5 and 6 where a significant jump is seen. It can be concluded that the pK_a of the imidazole nitrogen is ca. 5.5, similar to the value of 5.6 reported for the analogous binuclear complex, **4**.¹⁴

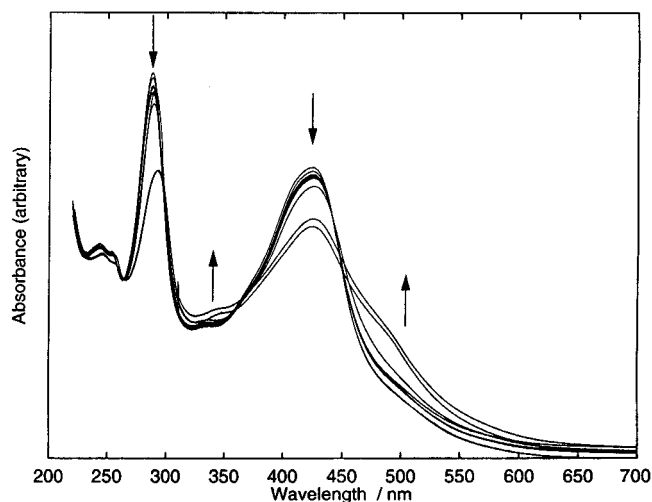
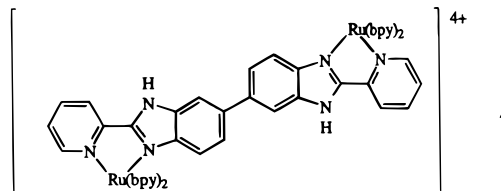


Figure 4. UV-vis spectra of the Ru(II) polymer complex **2** in phosphate-buffered aqueous methanol at pH values of 2.00, 2.23, 2.52, 2.69, 2.95, 3.82, 4.93, 6.21, 7.00, and 8.33. Arrows indicate changes with increasing pH.

Table 1. Characteristics of the IT Band for Polymer **2** and the Analogous Binuclear Complex, **4**

complex	ϵ_{max} ($\text{L mol}^{-1} \text{cm}^{-1}$)	ν_{max} (cm^{-1})	$\Delta\nu_{1/2}$ (cm^{-1})	H_{AB} (cm^{-1})
2 (film 1)	62	7742	2320	46
2 (film 2)	125	7294	2291	62
4 (ref 14)	~ 100	7300	3100	60–80



While transparent in the near-infrared in the Ru(II) state, oxidative spectroelectrochemistry of films of **2** exhibits new absorptions in this region. An intervalence transfer (IT) band was observed by the subtraction of one-half the intensity of the spectrum of the fully oxidized form from the spectrum of the half-oxidized form (both spectra having had the neutral state spectrum subtracted as a background),⁷ as reported for the binuclear complex, **4**.¹⁴ The degree of electronic coupling between neighboring metal sites, H_{AB} , evaluated by using eq 3,^{27,28} is similar to that in the binuclear complex (Table 1).

$$H_{\text{AB}} = (2.05 \times 10^{-2}) \left[\frac{\epsilon_{\text{max}} \Delta\nu_{1/2}}{\nu_{\text{max}}} \right]^{1/2} \left[\frac{\nu_{\text{max}}}{r} \right] \quad (3)$$

ν_{max} , $\Delta\nu_{1/2}$, and ϵ_{max} are the position, width at half-height, and extinction coefficient, respectively, of the IT band, and r is the distance (ca. 15 \AA)¹⁴ between metal centers.

Cyclic voltammetry of a thin film of the polymer complex **2** shows a number of interesting features. A redox wave due to the Ru(III/II) couple appears in the range of ca. 0.8 to 1.2 V vs SSCE, depending on the degree of protonation of the polymer backbone (Figure 5). This behavior is similar to that observed previously in binuclear ruthenium complexes bridged by benzimidazole-based ligands.¹⁴ The variation of the potential of this process indicates that the charge distribution on the polymer

(26) Pud, A. A. *Synth. Met.* **1994**, *66*, 1.

(27) Hush, N. S. *Progr. Inorg. Chem.* **1967**, *8*, 391.

(28) Creutz, C. *Progr. Inorg. Chem.* **1983**, *30*, 1.

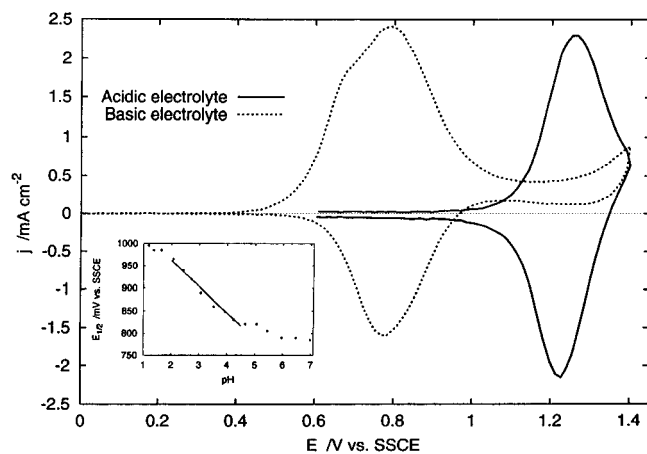


Figure 5. Cyclic voltammety (100 mV s^{-1}) of a thin ($\Gamma_{\text{Ru}} = 3.6 \times 10^{-8} \text{ mol cm}^{-2}$) film of **2** on a 0.0052 cm^2 Pt disk electrode in acetonitrile containing $0.1 \text{ M Et}_4\text{NClO}_4$ and ca. 50 mM HClO_4 (solid line) or ca. $5 \text{ mM Bu}_4\text{NOH}$ (dashed line). The inset shows the half-wave potential of the Ru(III/II) couple vs pH in an aqueous phosphate buffer.

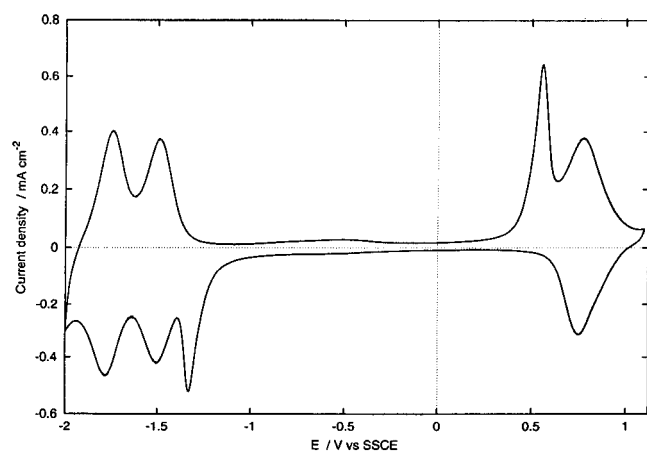


Figure 6. Steady-state cyclic voltammogram of **2** on a Pt disk electrode in neutral acetonitrile + $0.1 \text{ M Et}_4\text{NClO}_4$.

backbone, as dictated by the presence or absence of the imidazole proton, influences the electron density on the ruthenium center. The Ru(III/II) half-wave potential changes by -63 mV pH^{-1} in the pH 2–4 range, consistent with a one-proton, one-electron process (see inset in Figure 5).

Cycling over a broader range in neutral electrolyte gives a steady-state CV as shown in Figure 6. A pair of bipyridine-based reductions are present at -1.47 and -1.77 V vs SSCE , and the Ru(II/III) couple appears near its lower extreme, ca. 0.8 V , and varies slightly in position from film to film. A pair of pre-peaks, whose positions are variable, are also present, and we ascribe these to water in the film: sweeping the potential to below ca. -1.2 V reduces the water, generating OH^- and increasing the pH, while sweeping to positive potentials causes the oxidation of OH^- and water, and decreases the pH. Evidence for this explanation is given by the observations that (i) either pre-peak will only appear for one or two sweeps if the potential limits are set so the other is not accessed and (ii) the Ru(III/II) wave moves to higher potentials when the lower switching potential is made more positive than the reduction pre-peak (see Supporting Information). The addition of small quantities of water to the electrolyte solution has no effect on position or the magnitude of the pre-peaks, suggesting that the water involved in these processes is trapped in the polymer film, and originates before or during the casting process. This is consistent

with the tendency for benzimidazole-based polymers to absorb water tenaciously.¹³ Prepeaks observed for other redox polymers such a poly-Ru(vinyl-bpy)₃²⁹ may also be due to residual water. The advantage of the present system, from a diagnostic point of view, is that it shows that the pH within the polymer layer is changing. Similar pH changes presumably occur in the poly-Ru(vinyl-bpy)₃ system, and other Ru-bpy based polymers.

Electron Transport in the Ru Polymer, 2. One of the major reasons for preparing polymer **2** was to investigate the extent to which electronic communication between Ru centers through the conjugated polymer backbone would enhance electron transport in the polymer. Since the backbone of the polymer is not doped in the potential region of the Ru(III/II) formal potential, it does not contribute directly to the electronic conductivity of the polymer in this region. The rate of the Ru(III/II) redox process is therefore determined by the rate of electron exchange, or hopping, between redox sites. This is conveniently measured and represented as the electron diffusion coefficient, D_e .

In a preliminary report on this work,³⁰ we showed that D_e values for **2** from impedance measurements were significantly higher than values for poly[Ru(bpy)₂(4-vinylpyridine)₂], a similar but nonconjugated polymer. Furthermore, D_e for **2** was found to be higher in the presence of base, consistent with the stronger electronic coupling reported for the deprotonated model complex.¹⁴ These findings were criticized by reviewers of the original communication because of the use of impedance spectroscopy, a technique that has not been widely used for D_e measurements. We validate the impedance results here by comparing them with results from two more conventional techniques, rotating disk voltammetry and dual electrode voltammetry, and we also show that impedance spectroscopy is the most precise technique.

At the polymer complex's formal potential, complex plane (Nyquist) impedance plots of thin films of **2** show two distinct regions, as predicted by the finite transmission line model of Alberly et al.³¹ This behavior is consistent with other redox polymer systems.³² Representative plots in acidic and in basic electrolyte solutions are presented in Figure 7. Extrapolation of the high-frequency 45° region to the real (Z') axis gives a resistance R_{high} equal to the sum of uncompensated solution resistance R_s and the film's ionic resistance R_i . R_{low} is obtained similarly from the Z' intercept of the nearly vertical low-frequency region. R_e , the electronic resistance of the system, is given by eq 4:³¹

$$R_e = 3(R_{\text{low}} - R_{\text{high}}) \quad (4)$$

The low-frequency capacitance of the film C_{low} can be obtained from the slope of a plot of the imaginary impedance (Z'') vs $1/\omega$ (ω is frequency in rad s^{-1}). With the film thickness (d) determined as described earlier, the electron diffusion coefficient D_e may be found:³³

$$D_e = d^2/C_{\text{low}}R_e \quad (5)$$

It was found that a pretreatment of the films by soaking in electrolyte solution for ca. 20 min was necessary for good reproducibility. Repeat experiments on the same film invariably

(29) Denisevich, P.; Willman, K. W.; Murray, R. W. *J. Am. Chem. Soc.* **1981**, *103*, 4727.

(30) Cameron, C. G.; Pickup, P. G. *Chem. Commun.* **1997**, 303.

(31) Alberly, W. J.; Elliott, C. M.; Mount, A. R. *J. Electroanal. Chem.* **1990**, *288*, 15.

(32) Musiani, M. M. *Electrochim. Acta* **1990**, *35*, 1665.

(33) Mathias, M. F.; Haas, O. *J. Phys. Chem.* **1992**, *96*, 3174.

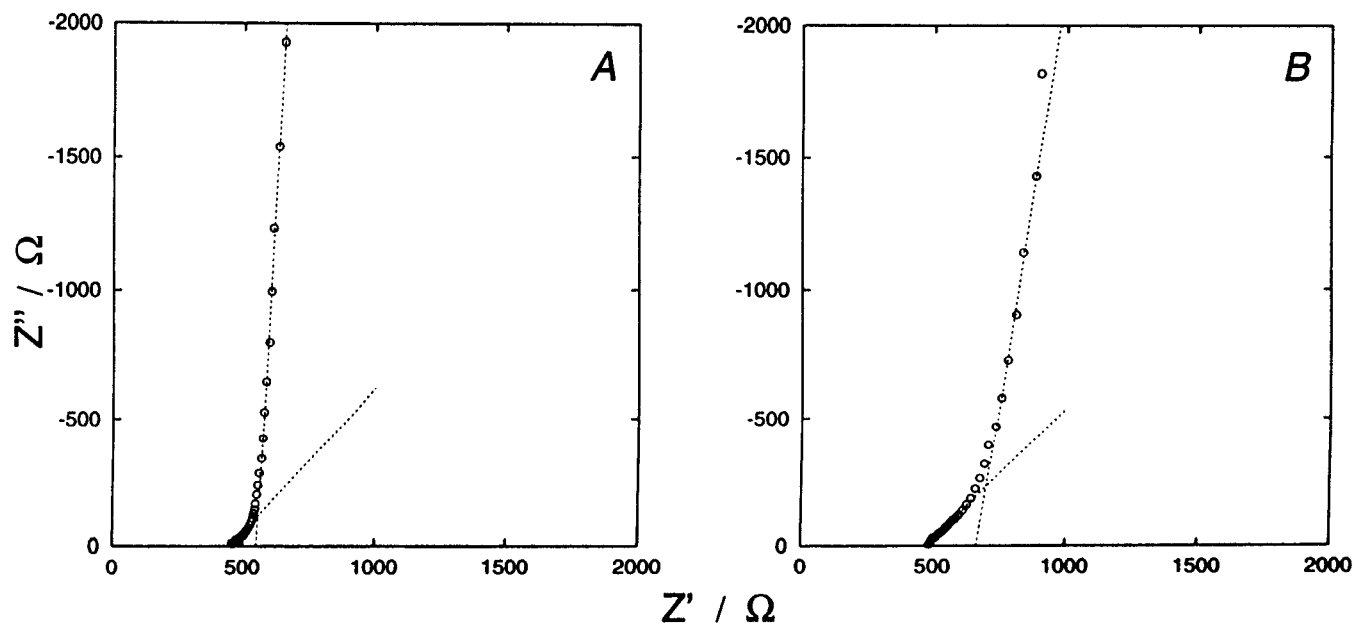


Figure 7. Typical complex plane impedance responses of a film of **2** in acetonitrile containing 0.1 M Et_4NClO_4 and (A) HClO_4 or (B) Bu_4NOH . DC offset potentials used were 1.200 and 0.775 V vs SSCE, respectively.

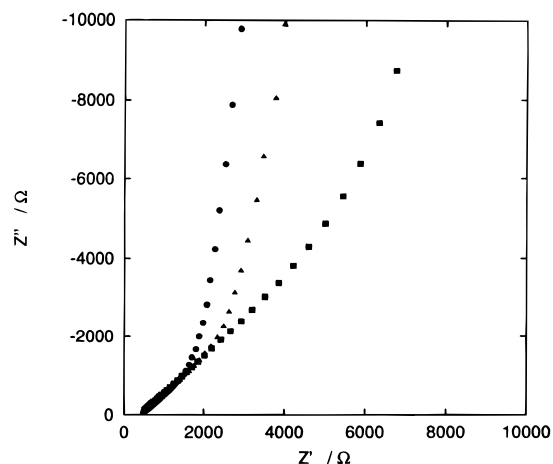


Figure 8. Degradation of impedance response at 1.200 V in a film of **2** in acetonitrile containing 0.1 M Et_4NClO_4 and acidified with HClO_4 .

showed decay of the measured D_e as shown in Figure 8. This degradation is consistent with the other methods, and can be attributed to the degradation of the polymer backbone in the course of long-term exposure to elevated potentials.

Another useful approach to measuring electron conduction or diffusion across a polymer film is the dual or “sandwich” electrode assembly.³⁴ A thin film of polymer is cast on a platinum disk electrode and a thin gold film is then vapor deposited over the top of the polymer film and a second disk electrode. The potential at each side of the polymer film may then be controlled with a bipotentiostat. The gold film is sufficiently porous to permit the motion of solvent and ions between the polymer film and solution bulk.

A representative current–voltage response is shown in Figure 9. The gold coating is held at a low potential, 0.6 V for example in acidified media, while the polymer-coated electrode is swept to increasingly positive values. At sufficiently high potentials, oxidized Ru(III) sites begin to accumulate near the Pt electrode surface. As the potential increases, a gradient forms between the oxidized Ru(III) sites near one electrode and the reduced

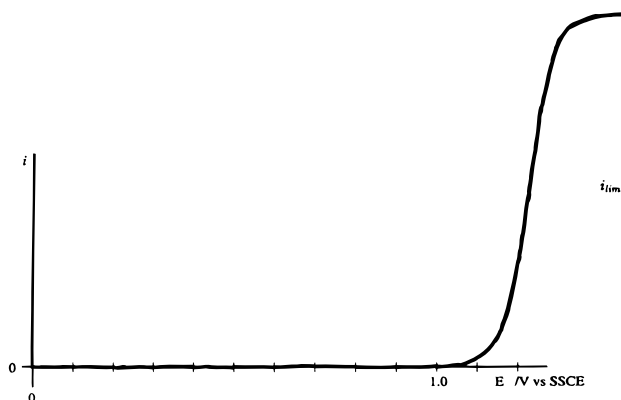


Figure 9. Typical current–voltage response for a Pt/polymer/Au sandwich electrode in acetonitrile containing 0.1 M Et_4NClO_4 and acidified with HClO_4 .

Ru(II) sites near the other. As these positive sites move through the film (or, conversely, as electrons move through it in the opposite direction) a current develops between the two electrodes. The limiting current that can develop as a result of this gradient is related to D_e as derived³⁴ from Fick’s first law and is described by

$$i_{\text{lim}} = nFAD_e C_{\text{Ru}}/d \quad (6)$$

d was determined by cyclic voltammetry following removal of the gold film with mercury. A high failure rate (>80%) was experienced with this method because it was difficult to obtain complete coverage of the Pt electrode with polymer, and swelling of the polymer tended to disrupt the gold coating.

D_e can also be measured in a film coating a rotating disk electrode in a cell containing some well-behaved electrochemically active donor species with $E_{1/2}$ at least several hundred millivolts less positive than that of the polymer film’s Ru(III/II) wave.³⁵ As the electrode potential is increased, oxidation of the metal centers from Ru(II) to Ru(III) spreads from the polymer–electrode interface. At the polymer–solution interface,

(34) Pickup, P. G.; Kutner, W.; Leidner, C. R.; Murray, R. W. *J. Am. Chem. Soc.* **1984**, *106*, 1991.

(35) Ikeda, T.; Leidner, C. R.; Murray, R. W. *J. Electroanal. Chem.* **1982**, *138*, 343.

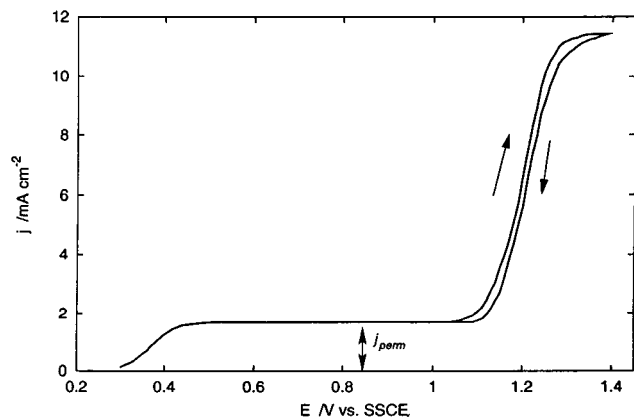


Figure 10. Typical RDE voltammogram in acetonitrile containing 0.1 M Et_4NClO_4 , ~ 7 mM ferrocene, and ~ 0.01 M HClO_4 of a Pt electrode coated with **2**. Scan rate = 10 mV s^{-1} , rotation rate = 2500 rpm .

an electron is accepted from the donor species. This electron then travels through the Ru(II) concentration gradient to the electrode. This condition allows for the measurement of the rate of electron flow from the solution to the electrode through the polymer film, and the characterization of this transport as a function of potential in a manner analogous to the sandwich electrode. The relationship between i_{lim} and D_e (in the absence of mass transport limitation) is given above in eq 6.

In the present case ferrocene was employed as the solution electron source. A typical current–voltage response is shown in Figure 10. A small baseline current due to ferrocene is evident at potentials above $E_{1/2}$ (ferrocene) and below $E_{1/2}$ (**2**) in all experiments and its relative magnitude varied randomly from film to film. This current is evidently due to ferrocene reacting directly at exposed regions of the Pt surface. It is not due to permeation through the polymer layer since it did not show any correlation with film thickness.

Directly measuring the limiting current during slow potential sweeps was found to be unsatisfactory since significant degradation of the current response resulted from extended and repeated exposures to elevated potential. An alternate approach utilizes the Nernst equation to extrapolate to i_{lim} from $i - E$ data at potentials below $E_{1/2}$ (eq 7 for $i \ll i_{\text{lim}}$). Avoiding high potentials in this manner extends the lifetime of the film almost indefinitely.

$$E - E_{1/2} = (RT/nF) \ln i - (RT/nF) \ln i_{\text{lim}} \quad (7)$$

From eq 7, a plot of $E - E_{1/2}$ against $\ln i$ in this potential region will give a straight line, as shown in Figure 11. $E_{1/2}$ was measured for each film used. The accuracy of this extrapolation was checked by comparing calculated limiting currents with the limiting currents measured at potentials significantly positive of $E_{1/2}$, which were sufficiently stable to make a reasonable comparison.

D_e results for the three methods in acidic and basic media are summarized in Table 2. There is good agreement between results measured in acid, although the dual electrode technique exhibits poor precision. The impedance method is therefore validated, and can be seen to be the most precise. Results in base were difficult to obtain except by impedance spectroscopy. Nonetheless, the one successful dual electrode voltammetry experiment does confirm the high D_e measured by impedance spectroscopy.

The enhancement of D_e when the polymer backbone is deprotonated parallels the observed increase in inter-metal coupling previously reported in the binuclear analogues, and

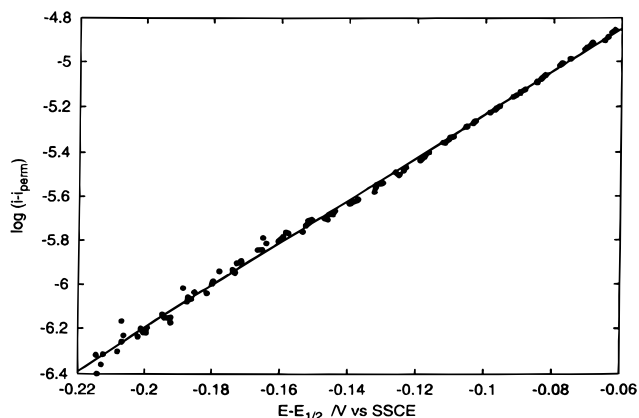


Figure 11. Log current vs $E - E_{1/2}$ plot for data from a RDE experiment similar to that depicted in Figure 10.

Table 2. D_e Results ($\text{cm}^2 \text{ s}^{-1}$) and Standard Deviations (s) for **2**

method	acid		base	
	D_e	s (n)	D_e	s (n)
dual electrode	5.5×10^{-9}	4.7×10^{-9} (2)	4.2×10^{-8}	(1)
RDE	5.4×10^{-9}	2.6×10^{-9} (4)		
impedance	6.9×10^{-9}	1.6×10^{-9} (3)	1.0×10^{-8}	0.1×10^{-8} (2)

indicates that metal valence transfer occurs through the polymer backbone. Furthermore, the D_e values obtained for **2** are much higher than those for similar ruthenium polymer systems where the metal cannot interact with a conjugated backbone. For example, D_e is only $7 \times 10^{-10} \text{ cm}^2 \text{ s}^{-1}$ for poly[Ru(bpy)₂(4-vinylpyridine)₂]^{3+/2+},³⁴ and only $2 \times 10^{-10} \text{ cm}^2 \text{ s}^{-1}$ for poly[Ru(bpy)₂(3-{pyrrol-1-ylmethyl}pyridine)₂]^{3+/2+}.³⁶

Conclusions

The results show for the first time that electron transport between metal centers is enhanced significantly when the metal sites are coordinated directly to the π -backbone of a conjugated polymer. Rates of electron diffusion in the present system are more than a factor of 10 greater than those in similar ruthenium systems where the metal is electronically isolated by saturated bonds.

It was found that the electron diffusion coefficient varied significantly depending on whether the polymer backbone was protonated, and also showed degradation as the backbone suffered damage from exposure to elevated potentials. The electron diffusion cannot be ascribed to the π chain alone as it has been shown that the uncomplexed polymer is electrochemically inactive at the corresponding potentials in acidic and basic media. Rather, it is presumed that the electronic interaction between metal centers through the backbone, as demonstrated by an intervalence charge-transfer band in the NIR spectrum, is responsible for the enhanced transport.

Acknowledgment. This work was supported by the Natural Sciences and Engineering Research Council of Canada and Memorial University.

Supporting Information Available: Proton NMR spectra of **1** and **3**, and cyclic voltammograms of **2** following a single scan through the reduction pre-peak (PDF). This material is available free of charge via the Internet at <http://pubs.acs.org>.

JA9843472